Computational fluid dynamics confirms drag reduction associated with trilobite queuing behaviour

Hanchen Song[1], Haijun Song[1]*, Imran A. Rahman[2], Daoliang Chu[1]

[1]*State Key Laboratory of Biogeology and Environmental Geology, School of Earth Sciences, China University of Geosciences, Wuhan 430074, PR China*

[2]*Oxford University Museum of Natural History, Parks Road, Oxford, OX1 3PW, UK*

E-mail addresses: haijunsong@cug.edu.cn (Haijun Song)

Abstract

Queuing behaviour has been documented in marine arthropods from Cambrian to modern oceans. It was previously hypothesized that this behaviour provided energy savings through hydrodynamic drafting, with trilobites in following positions hypothesized to produce less drag than those leading. In this study, we evaluate the hydrodynamics of queuing behaviour in the Devonian trilobite *Trimerocephalus chopini* using computational fluid dynamics. The results show that the drag forces of the trilobites following in the queue were substantially lower than those produced by the leader (~65–79% lower at velocities of 0.5–2 cm s^{-1}). Drag reduction was positively correlated with the movement speed of the trilobites, but decreased with increasing distance from the leader, and there was essentially no drag reduction at all for the first following trilobite when the following distance was greater than about six times its

body length. This agrees with fossil evidence preserving trilobites in queues in close proximity to each other. The results also show that drag reduction was still significant (~86.8% at 2 cm s^{-1}) even for the longest queues preserved in the fossil record. Our findings support the hypothesis that the queuing behaviour of trilobites was an adaptation for reducing hydrodynamic drag. This drag reduction effect compensated for the energy cost of movement, which would have been particularly advantageous during migration.

Key words: trilobite; queuing behaviour; computational fluid dynamics; drag reduction.

Introduction

Elucidating the behaviours of ancient organisms is a major research focus in palaeontology. Although much of this work relies on comparison with extant analogues, under unusual conditions the fossil record can provide direct insights into past lifestyles (Benton 2010). Perhaps the most common such evidence comes in the form of trace fossils, e.g., (Bromley 1996), but body fossils can also capture certain behaviours. One example of this is queuing behaviour, which can be inferred where individuals are preserved in ordered rows.

The oldest evidence of queuing by arthropods in the fossil record are the chain-like associations of the putative crustacean *Synophalos xynos*, which have been described from the Cambrian (~518 Ma) Chengjiang Lagerstätte of Yunnan, China (Hou et al., 2009). Queuing behaviour has also been documented for trilobites throughout the Palaeozoic (Fig. 1). The oldest records date back to the Lower

Ordovician (~480 Ma) and consist of queues of *Ampyx priscus* from the Fezouata Shale of Morocco (Vannier *et al.* 2019). Other trilobites thought to form queues include *Agerina* and *Ampyx* from the Lower Ordovician Zini Formation of Morocco (Chatterton *et al.* 2008) and *Bathycheilus*, *Retamaspis* and/or *Salterocoryphe* from Middle Ordovician roofing slates in Portugal (Gutiérrez-Marco *et al.* 2009). Perhaps most strikingly, numerous examples of well-preserved, single-file queues of *Trimerocephalus chopini* have been reported from the Upper Devonian (~365 Ma) Kowala Quarry of Poland (Radwański *et al.* 2009; Kin & Błażejowski 2013; Błażejowski *et al.* 2016).

Based on comparisons with modern marine arthropods exhibiting similar queuing behaviours, such as spiny lobsters, the queues of trilobites from the Devonian of Poland have been interpreted to be the result of mass migrations (Błażejowski *et al.* 2016). It has been suggested that these queues were controlled by chemotaxis, with trilobites moving after one another in response to chemical signals (Błażejowski et al., 2016). However, an alternative hypothesis is that the queuing behaviour of trilobites is linked to drag reduction, analogous to bicycle pelotons where cyclists following the leader encounter lower drag (Trenchard *et al.* 2017). To test this hypothesis, we constructed a three-dimensional digital model of *Trimerocephalus chopini* and used this to create a virtual queue of trilobites (Song et al. 2021). We then used computational fluid dynamics (CFD) to quantify drag forces for each of the models within this queue. The results agree with the findings of (Trenchard *et al.* 2017), suggesting that trilobites formed single-file queues to save energy or move at higher speeds for longer periods of time.

Material and method

Three-dimensional modelling

Trimerocephalus chopini is known from the Upper Devonian (Famennian) of Kowala Quarry, near Kielce in south central Poland (Kin & Błażejowski 2013). At this locality, queues of trilobites are preserved in horizons of marly shales with occasional calcareous concretions (Radwański *et al.* 2009). Trilobites are aligned with each individual in the same orientation and with adjacent individuals in close contact or partly overlapping one another (Radwański *et al.* 2009; Błażejowski *et al.* 2016).

Through reference to published images and reconstructions (Berkowski 1991), we constructed an idealized three-dimensional digital model of the trilobite *Trimerocephalus chopini* (Fig. 2). Modelling was performed with Unigraphics NX (v. 12.0), a computer-aided design program, using reconstructions of the morphologically similar species *Trimerocephalus interruptus* as a base. The shape of the model was then adjusted by reference to images of *Trimerocephalus chopini*, with appendages (i.e., antennae and legs) excluded to minimize model complexity (Fig. 2). The final model is 30 mm long, 18 mm wide and 9 mm high (Fig. 3A, B).

The model of *Trimerocephalus chopini* was used to create a virtual queue of trilobites (Fig. 3C). Known fossil examples of queuing trilobites range from a few to more than 20 individuals (Radwański *et al.* 2009; Kin & Błażejowski 2013, 2013; Błażejowski *et al.* 2016); we created a queue consisting of four individuals, which was deemed sufficient to evaluate the hydrodynamics of queuing behaviour while at the same time ensuring our simulations were computationally feasible. Individuals were arranged in a row facing in the same direction and were placed 10 mm apart from each

other, a spacing equal to about one third the body length of the trilobites, as shown in fig. 3 of Radwański *et al.* (2009).

Computational fluid dynamics

CFD simulations were carried out in ANSYS Fluent (v. 19.2). The computational domain consisted of a three-dimensional rectangle. The virtual queue of trilobites was placed 2 mm above the lower boundary of the domain, accounting for the presence of appendages (not digitally modelled) that would have raised individuals slightly about the sediment surface. Because the models are bilaterally symmetrical, the queue was cut along the plane of symmetry (thereby reducing the complexity of the simulations). Sensitivity tests were undertaken to determine the optimal domain size, and based on these we selected a domain measuring 780 mm in length, 175 mm in width and 132.5 mm in height, with the queue positioned with the first individual 135 mm away from the front end of the domain (Fig. 4). The queue was then subtracted from the domain using a Boolean operation. The results of sensitivity analyses are provided as supplementary material. Using the local encryption method, we created a wedge-like body of influence (Figs. 4, 5) based on the thickness of the boundary layer area estimated from the von Karman boundary-layer momentum integral equation, which fully encompassed the boundary layer. Model defects were then cleaned in ANSYS SCDM, which involved removing short sides, merging complex surfaces, and filling holes.

The domain was meshed in ANSYS Fluent Meshing. An unstructured mesh was used to better capture the geometric complexity of the trilobite models. Sensitivity tests

were carried out to determine the optimal mesh size for use in CFD simulations. Close to the trilobite models, the minimum element size was 0.03 mm and the maximum element size was 0.15 mm, while within the body of influence more broadly the maximum element size was 0.6 mm. Across the computational domain, the minimum element size was 0.15 mm and the maximum element size was 8 mm, with a growth rate of 1.2 and a curvature normal angle of 10. The final mesh consisted of 2.93 million elements (Fig. 6).

Next, boundary conditions were assigned to the computational domain. A velocity inlet boundary was used to define the flow velocity at the front end of the domain, with an outflow boundary used to model the exit of the flow at the opposing end. Based on the range of movement speeds estimated for trilobites by Trenchard et al. (2017), we selected inlet velocities of 0.5, 1, 1.5 and 2 cm s^{-1} (Reynolds numbers of 149, 298, 447 and 597, respectively). Slip and symmetry boundary conditions were assigned to the top and sides of the domain, with no-slip boundary conditions assigned to the surfaces of the trilobite models and the lower surface of the domain (except for just in front of the queue, where a slip boundary condition was used to prevent the flow prematurely decelerating near the bottom due to viscous forces).

To evaluate the impact of distance from the leader on the results, simulations were performed for a queue of two individuals with the first following trilobite at distances of 0–45 cm from the leader using an inlet velocity of 2 cm s^{-1}. In order to account for the excess drag reduction caused by the deceleration of the bottom boundary layer in the spacing between the follower and the leader, a series of simulations were carried out with only a single trilobite at distances of 0–48 cm from the original position of the leader; we then interpolated the results between these distances at intervals of 0.1

cm using the linear interpolation method. This excess drag reduction and the system error caused by the removal of the leader (average of the values at which the drag reduction, after subtracting the excess drag, did not change with increasing following distance) were then subtracted from the results.

To test whether drag reduction effects would be significant in the longest queues of *Trimerocephalus chopini* described in the fossil record (Błażejowski *et al.* 2016), a simulation was undertaken with 20 individuals placed 0 mm apart from each other (spacing based on figs. 2, 3 in Błażejowski *et al.* (2016)) using an inlet velocity of 2 cm s^{-1}.

Based on the calculated range of Reynolds numbers (which are within the laminar flow regime) and the low-energy palaeoenvironment inferred for *Trimerocephalus chopini* (Błażejowski et al. 2016), we selected a laminar model for use in all our simulations. A double-precision, stationary solver was run in six parallel threads. The governing equations were solved using the SIMPLEC algorithm, adopting a second-order upwind discretization scheme. Simulations were run until convergence of residual error to less than 10^{-4}. The results were visualized as false-colour plots of velocity and pressure. In addition, drag forces were obtained for each of the trilobite models in the virtual queue. Drag coefficients (C_D) were calculated using the following formula:

$$C_D = \frac{2F_D}{\rho U^2 A} \quad (1)$$

where F_D is the drag force, ρ is the density of seawater (998.2 kg m^{-3}), U is the inlet velocity (cm s^{-1}) and A is the characteristic area (m^2). Calculations were repeated with both the projected frontal area and the total surface area taken as the characteristic area.

Results

Drag forces and coefficients

The drag forces of the trilobites within the queue of four individuals (with distances of 1 cm between adjacent trilobites) increased with increasing inlet velocity (Table 1; Fig. 7A). In all cases, the drag forces of the following trilobites were lower than the leader. The drag forces produced by the first follower were typically the lowest, with the drag forces increasing as the position of the trilobite within the queue increased (apart from at the lowest inlet velocity of 0.5 cm s^{-1}).

Substantial drag reduction compared to the leader (Table 1; ~65–79%) was observed for the trilobites in the following positions at all simulated inlet velocities (Fig. 7B). The percentage drag reduction increased with inlet velocity; at the highest inlet velocity of 2 cm s^{-1}, the drag forces of the followers were an average of 75% lower than the leader.

Drag coefficients calculated using either the projected frontal area or total surface area as the characteristic area showed the same general pattern. In both cases, the drag coefficients of the trilobites within the queue decreased with increasing inlet velocity, and the drag coefficients of the followers were always lower than the leader (Fig. 8).

Flow patterns

Velocity decreased as the flow approached the trilobite models, with a sharp negative gradient developed near to the models and the no-slip lower boundary of the domain. Additionally, a region of low velocity flow was developed downstream of the trilobite models (Fig. 9A).

The highest pressures were concentrated at the upstream ends of the trilobite models for each individual in the queue, and were substantially higher at the front end of the leader (Fig. 9B).

Drag reduction at different distances from the leader

Without subtracting the excess reduction, the percentage drag reduction of the trilobite in the first following position decreased up to a following distance of about 9 cm, and then increased with increasing distance from the leader (Fig. 10A). The excess drag reduction caused by the deceleration of the bottom boundary layer in the spacing between the follower and the leader increased with increasing distance from the original position of the leader (Fig. 10A, B). After subtracting the excess reduction from the results, the percentage drag reduction decreased up to a following distance of about 18 cm, and was then largely invariant (less than 1% difference over following distances of 18–45 cm) with increasing distance from the leader (Fig. 10C). After subtracting both the excess reduction and the systematic error, drag reduction was found to be ~86% when the distance between the leader and the first follower was 0 cm, decreasing to a minimum (~0%) at a following distance of greater than ~18 cm (Fig. 10D).

Drag forces and coefficients for queue of 20 individuals

In the queue of 20 individuals (with distances of 0 cm between adjacent trilobites), drag forces of all the following trilobites were significantly lower than the leader (Fig. 11A). The drag force produced by the first follower was the lowest, with the average percentage drag reduction of each following trilobite 86.8%. Drag coefficients calculated using either the projected frontal area or total surface area as the characteristic area showed the same general pattern to the drag forces (Fig. 11B, C). Drag coefficients of all the following trilobites were lower than the leader, and these values were lowest for the trilobite in the first following position.

Discussion

The results of our CFD simulations show that the drag forces and coefficients produced by trilobites in the following positions in the queue were much lower than the leader (Table 1; Figs. 7, 8), supporting the hypothesis that forming queues reduced the drag they experienced during locomotion (Trenchard *et al.* 2017). Our results agree with Trenchard et al. (2017), who approximated drag forces for trilobites in queues and found that the drag was lowest for following individuals across a range of travelling speeds (0–2 cm s^{-1}). Reducing drag by forming queues is thought to help conserve energy in extant spiny lobsters (Bill & Herrnkind 1976), and the same was probably true for queuing trilobites; Trenchard et al. (2017) estimated energy savings of 61.5% for trilobites in the following positions (compared to solitary individuals). Moving in

queues would therefore have considerably reduced the energetic demands of following trilobites.

This drag reduction effect increased with increasing inlet velocity, up to an average of ~75% at 2 cm s^{-1} in the queue of four individuals spaced 1 cm apart (Table 1; Fig. 7B). Thus, queuing behaviour would have provided greater benefits in terms of drag reduction at higher travelling speeds within the range of 0–2 cm s^{-1}. Furthermore, drag reduction may be closely linked to energy savings. Crouch *et al.* (2017) showed that the power-output reductions of following riders in queues of four cyclists were very similar to the magnitude of the drag reduction. Moreover, Broker *et al.* (1999) found that the percentage power reduction in cyclists in following positions was similar to the reduction in their energy consumption. Similarly, Chatard & Wilson (2003) suggested that the drag reduction provided by swimming behind or to the side of another swimmer was responsible for an energy saving. However, the exact relationship between drag reduction and the associated energy saving varies. One reason for this is that there are some other factors not affected by drag reduction. For instance, in runners the following individual experiences an 80% reduction in wind resistance but only a 6% reduction in the total energy cost (Pugh 1971), in part due to the braking forces during foot-strikes and because other biomechanical factors required most of the power outputs (Nummela *et al.* 2007) . And for cyclists, rolling resistance is not affected by aerodynamic drag reduction leading to a reduction in wind resistance of about 38% and a decrease in the power required of about 33% for two cyclists traveling in a line at 11.1 m s^{-1} (Kyle 1979). Thus, in order to link the total energy saving per second (represented by power output) with the drag reduction of the following individuals, it is necessary to estimate the power output caused by drag relative to the total power output. We employed an

alternative method using metabolic rate. The metabolic rate of extant arthropods is one of the main indexes reflecting total energy consumption and is known to be a function of body weight (Equation 2) (Reichle 1968).

$$P_M = 0.32 \times BW^{0.84} \quad (2)$$

Where P_M is the metabolic rate of arthropods (μl O_2 h^{-1}) and BW is the body weight (mg).

In addition, the body weight of arthropods is a function of the body length (Equation 3) (Sohlström *et al.* 2018).

$$\log_{10}(BW) = -0.792 + 2.181 \times \log_{10}(BL) \quad (3)$$

Where BW is the body weight in mg, and BL is the body length with mm.

Based on equations 2 and 3, the metabolic rate of arthropods can therefore be shown to be a function of the body length (Equation 4).

$$P_M = 0.32 \times \left[10^{-0.792+2.181\times\log_{10}(30)}\right]^{0.84} \quad (4)$$

BL of our trilobite model is 30 mm. Thus, the estimated P_M is 35.16 μl O_2 h^{-1}, which is equal to 9.77×10^{-3} μl O_2 s^{-1}, and this reflects the total energy consumption of each trilobite. The decreasing power output caused by drag reduction (P_{DR} in J s^{-1}) (Equation 5) can be calculated as follows:

$$P_{DR} = DR \times F_D \times U \quad (5)$$

Where DR is the percentage average drag reduction of the following trilobites (%), F_D is the drag force of the leader (N), and U is the speed of trilobites (m s^{-1}).

Thus, the energy saving provided by drag reduction in each following trilobite

relative to the total energy consumption can be expressed as P_{DR} / P_M (J μl^{-1} O_2). In the queue of four individuals with a following distance of 1 cm and at a speed of 2 cm s^{-1}, $P_{DR} / P_M = 1.25 \times 10^{-5}$ J μl^{-1} O_2. In the queue of 20 individuals with a following distance of 0 cm and at a speed of 2 cm s^{-1}, $P_{DR} / P_M = 1.42 \times 10^{-5}$ J μl^{-1} O_2. In animals, the energy equivalents of oxygen consumption vary with diet (Elliott & Davison 1975), and it is therefore difficult to estimate the percentage energy saving provided by drag reduction. Nevertheless, P_{DR} / P_M appears to be a useful measure for comparing trilobites to other arthropods and other kinds of energy saving mechanism.

The variation range hypothesis proposed by Trenchard & Perc (2016) and Trenchard *et al.* (2017) implies a correlation between the size range of trilobites in queues and the percentage energy saving. Based on the discussion above, it seems likely the energy saving provided by drag reduction was lower than the percentage drag reduction (~75% in the queue of 4 individuals with following distance of 1 cm at 2 cm s^{-1}). The size range of trilobites in queues of *Trimerocephalus chopini* reported by Błażejowski *et al.* (2016) is about 63%, consistent with the predictions of the variation range hypothesis (Trenchard et al. 2017).

We proposed that trilobites might have preferentially chosen to form single-file queues when moving quickly to conserve energy (Trenchard et al. 2017). In contrast, disordered groups may have been more common when trilobites were travelling at slower speeds. As suggested by Trenchard et al. (2017), the leader could have been a stronger individual, capable of higher sustained speeds, with the weaker followers able to maintain the same speed due to the energy saving benefits of their position in the queue. Alternatively, trilobites might have taken it in turns to assume the high-drag

leading position, with the leader periodically retreating into a following position in order to conserve energy (Trenchard et al. 2017). This is analogous to groups of cyclists (i.e., bicycle pelotons), in which riders move in a single-file queue, alternating between leading positions, to maximize their sustainable metabolic capacities (McCole *et al.* 1990; Trenchard *et al.* 2017; Blocken *et al.* 2018). Regardless of the exact energy saving mechanism, however, queuing behaviour of this kind would in all likelihood have enabled groups of trilobites to move at higher speeds for longer periods (Trenchard et al. 2017). This would have been especially beneficial during migration, which has been hypothesized for *Trimerocephalus chopini*.

Błażejowski et al. (2016) argued that chemotaxis was a key control on queues of blind trilobites such as *Trimerocephalus chopini*. However, Trenchard et al. (2017) suggested that the energy savings of queues preceded the evolution of a chemosensory apparatus; this agrees with Wang *et al.* (2014), who demonstrated that hydrodynamic drafting can lead to collective behaviour even in inanimate particles in the liquid. Furthermore, cells of the slime mold *Dictyostelium discoideum* have also been proposed to form queues in the absence of chemotaxis in order to conserve energy (Trenchard 2019). Hence, it is likely that chemotaxis was a derived character of *Trimerocephalus chopini*. Nevertheless, we propose that both drag reduction and chemotaxis played important roles in trilobite queuing behaviour, with chemical signals providing the stimulus for individuals to find and follow each other, while drag reduction and the associated energy savings represented one of the main benefits of doing so. Another possible benefit of queuing behaviour could be enhanced defence against predators; single-file queues of extant spiny lobsters are thought to provide protection for the

vulnerable abdomens of individuals (Herrnkind 1969), and a similar defensive function could have been beneficial for protecting the delicate appendages of trilobites.

Our results confirm that the shorter the distance between the leader and the first following trilobite in a queue, the greater the reduction in drag, and there was essentially no drag reduction at all for the first following trilobite when the following distance was greater than ~18 cm (i.e. about six times the body length of the trilobite) (Fig. 10). Several examples of queuing trilobites preserved in the fossil record show individuals in very close proximity (less than half the body length), including head-to-tail contact (Radwański *et al.* 2009; Błażejowski *et al.* 2016), and similar close associations are documented in other fossil (Hou *et al.* 2009) and modern (Herrnkind 1969) arthropods. For example, *Ampyx priscus* from the Lower Ordovician of Morocco formed queues with short inter-individual distances of less than twice its body length; it had long projecting spines, which might have helped maintain close physical contact between neighbouring individuals in a queue (Vannier *et al.* 2019), thereby achieving the greatest possible drag reduction. *Trimerocephalus chopini* lacked potential touch sensors, but as noted above might have been able to sense surrounding individuals through chemotaxis (Błażejowski *et al.* 2016). The results of our analyses show that trilobites could obtain greater than 61.3% drag reduction by ensuring following distances were less than half their total body length, similar to the queues reported by Radwański *et al.* (2009). We also find more than 19% drag reduction for trilobites with inter-individual distances of less than twice the body length, like those in the queue of *Ampyx priscus* reported by Vannier *et al.* (2019) (although the substantial morphological differences between *Ampyx priscus* and *Trimerocephalus chopini* mean this estimate might not be accurate for the former species). Nevertheless, we speculate

based on our results that following distances in queues of trilobites would need to be less than six times the body length in order to achieve any drag reduction effect.

We find that even in a very long queue consisting of 20 individuals in head-to-tail contact, all the following trilobites showed significant drag reduction compared to the leader (Fig. 11). The maximum number of *Trimerocephalus chopini* individuals preserved in the 78 examples of queues described by Błażejowski *et al.* (2016) is 19. This is consistent with our finding that queues of this size provided considerable drag reduction for all individuals. Considering that the average drag reduction across a queue of 20 individuals (~86.8%) was very similar to a queue of two individuals with a following distance of 0 cm (~86.2%), it is plausible that trilobites formed even longer queues than reported thus far.

The CFD simulations did not incorporate the effects of high-velocity turbulent currents, such as those associated with storm events, which would be expected to have influenced the hydrodynamic performance of queuing trilobites. The presence of occasional hummocky cross stratification in the sediments preserving *Trimerocephalus chopini* indicates storm activity might have periodically affected the trilobites (Błażejowski *et al.* 2016). However, this was most likely the cause of their mortality, stirring up anoxic, sulphide-rich sediment that killed the animals through suffocation, hypercapnia and/or toxic seawater (Błażejowski *et al.* 2016), rather than being representative of the normal conditions they inhabited.

These occasional, perhaps seasonal storms provide a possible explanation for the migratory behaviour of *Trimerocephalus chopini*. Environmental stress has been suggested as a potential cause of mass migrations of spiny lobsters (Herrnkind 1969), and storm events could have created a similar environmental pressure driving the

migration of trilobites (Błażejowski *et al.* 2016). Seasonal variations in temperature, ocean currents and food availability are other important factors that could have played a role. The hypothesized long-distance migrations of trilobites (Błażejowski *et al.* 2016) in the face of such environmental pressures would have been energetically demanding, but our results suggest this may have been partly compensated for by energy savings from drag reduction as the trilobites moved in queues.

Acknowledgments

We thank Javier Álvaro, Sally Thomas and two anonymous reviewers for helpful comments on an earlier version of this manuscript. This research was supported by the National Natural Science Foundation of China (41821001) and the National Mineral Rock and Fossil Specimens Resource Center, China. This is Center for Computational & Modeling Geosciences publication number 3.

Data Archiving Statement

Data for this study are available in the Dryad Digital Repository: https://doi.org/10.5061/dryad.n8pk0p2tv

References

BERKOWSKI, B. 1991. A blind phacopid trilobite from the Famennian of the Holy Cross Mountains. *Acta Palaeontologica Polonica*, **36** (3), 255–264.

BILL, R. G. and HERRNKIND, W. F. 1976. Drag Reduction by Formation Movement in Spiny Lobsters. *Science*, **193** (4258), 1146.

BŁAŻEJOWSKI, B., BRETT, C. E., KIN, A., RADWAŃSKI, A. and GRUSZCZYŃSKI, M. 2016. Ancient animal migration: a case study of eyeless, dimorphic Devonian trilobites from Poland. *Palaeontology*, **59** (5), 743–751.

BLOCKEN, B., VAN DRUENEN, T., TOPARLAR, Y., MALIZIA, F., MANNION, P., ANDRIANNE, T., MARCHAL, T., MAAS, G.-J. and DIEPENS, J. 2018. Aerodynamic drag in cycling pelotons: New insights by CFD simulation and wind tunnel testing. *Journal of Wind Engineering and Industrial Aerodynamics*, **179**, 319–337.

BROKER, J. P., KYLE, C. R. and BURKE, E. R. 1999. Racing cyclist power requirements in the 4000-m individual and team pursuits. *Medicine and Science in Sports and Exercise*, **31** (11), 1677–1685.

BROMLEY, R. G. 1996. Trace Fossils: Biology, Taphonomy and Applications. *Chapman & Hall London*, 361.

CHATARD, J.-C. and WILSON, B. 2003. Drafting distance in swimming. *Medicine and Science in Sports and Exercise*, **35** (7), 1176–1181.

CHATTERTON, B. D.E., FORTEY, R. A., RÁBANO, I., GOZALO, R. and

GARCÍA-BELLIDO, D. 2008. Linear clusters of articulated trilobites from Lower Ordovician (Arenig) strata at Bini Tinzoulin, north of Zagora, southern Morocco. *Advances in trilobite research. Cuadernos del Museo Geominero*, **9**, 73–77.

CROUCH, T. N., BURTON, D., LABRY, Z. A. and BLAIR, K. B. 2017. Riding against the wind: a review of competition cycling aerodynamics. *Sports Engineering*, **20** (2), 81–110.

ELLIOTT, J. M. and DAVISON, W. 1975. Energy equivalents of oxygen consumption in animal energetics. *Oecologia*, **19** (3), 195–201.

GUTIÉRREZ-MARCO, J. C., SÁ, A. A., GARCÍA-BELLIDO, D. C., RÁBANO, I. and VALÉRIO, M. 2009. Giant trilobites and trilobite clusters from the Ordovician of Portugal. *Geology*, **37** (5), 443–446.

HERRNKIND, W. F. 1969. Queuing Behavior of Spiny Lobsters. *Science*, **164** (3886), 1425.

HOU, X., SIVETER, D. J., ALDRIDGE, R. J. and SIVETER, D. J. 2009. A new arthropod in chain-like associations from the Chengjiang lagerstätte (lower Cambrian), Yunnan, China. *Palaeontology*, **52** (4), 951–961.

KIN, A. and BŁAŻEJOWSKI, B. 2013. A new Trimerocephalus species (Trilobita, Phacopidae) from the Late Devonian (Early Famennian) of Poland. *Zootaxa*, **3626** (3), 345–355.

KYLE, C. 1979. Reduction of Wind Resistance and Power Output of Racing Cyclists and Runners Travelling in Groups. *Ergonomics*, **22**, 387–397.

MCCOLE, S. D., CLANEY, K., CONTE, J. C., ANDERSON, R. and

HAGBERG, J. M. 1990. Energy expenditure during bicycling. *Journal of Applied Physiology*, **68** (2), 748–753.

NUMMELA, A., KERÄNEN, T. and MIKKELSSON, L. O. 2007. Factors related to top running speed and economy. *International Journal of Sports Medicine*, **28** (8), 655–661.

PUGH, L. G. C. E. 1971. The influence of wind resistance in running and walking and the mechanical efficiency of work against horizontal or vertical forces. *The Journal of Physiology*, **213** (2), 255–276.

RADWAŃSKI, A., KIN, A. and RADWAŃSKA, U. 2009. Queues of blind phacopid trilobites Trimerocephalus: A case of frozen behaviour of Early Famennian age from the Holy Cross Mountains, Central Poland. *Acta Geologica Polonica*, **59** (4), 459–481.

REICHLE, D. 1968. Relation of Body Size to Food Intake, Oxygen Consumption, and Trace Element Metabolism in Forest Floor Arthropods. *Ecology*, **49** (3), 538–542.

SOHLSTRÖM, E. H., MARIAN, L., BARNES, A. D., HANEDA, N. F., SCHEU, S., RALL, B. C., BROSE, U. and JOCHUM, M. 2018. Applying generalized allometric regressions to predict live body mass of tropical and temperate arthropods. *Ecology and Evolution*, **8** (24), 12737–12749.

Song, H.-C., Song, H.-J., Rahman, I., Chu, D.-L. 2021. Data from: Computational fluid dynamics confirms drag reduction associated with trilobite queuing behaviour, *Dryad Digital Repository*. https://doi.org/10.5061/dryad.n8pk0p2tv

TRENCHARD, H. 2019. Cell pelotons: A model of early evolutionary cell sorting, with application to slime mold Dictyostelium discoideum. *Journal of Theoretical Biology*, **469**, 75–95.

TRENCHARD, H., BRETT, C. E. and PERC, M. 2017. Trilobite 'pelotons': possible hydrodynamic drag effects between leading and following trilobites in trilobite queues. *Palaeontology*, **60** (4), 557–569.

TRENCHARD, H. and PERC, M. 2016. Energy saving mechanisms, collective behavior and the variation range hypothesis in biological systems: A review. *Biosystems*, **147**, 40–66.

VANNIER, J., VIDAL, M., MARCHANT, R., EL HARIRI, K., KOURAISS, K., PITTET, B., EL ALBANI, A., MAZURIER, A. and MARTIN, E. 2019. Collective behaviour in 480-million-year-old trilobite arthropods from morocco. *Scientific Reports*, **9** (1), 14941.

WANG, L., GUO, Z. L. and MI, J. C. 2014. Drafting, kissing and tumbling process of two particles with different sizes. *Computers & Fluids*, **96**, 20–34.

Figure/table captions

FIG. 1. Queuing behaviour in marine arthropods. A, chain-like associations of the putative crustacean *Synophalos xynos* from the Chengjiang Lagerstätte, China (Hou *et al.* 2009). B, queues of the trilobites *Agerina* and *Ampyx* from the Fezouata Shale, Morocco (Chatterton et al., 2008; Vannier et al., 2019). C, queues of the trilobites *Bathycheilus*, *Retamaspis* and/or *Salterocoryphe* from Portugal (Gutiérrez-Marco *et al.* 2009). D, queues of the trilobite *Trimerocephalus chopini* from Kowala Quarry, Poland (Radwański *et al.* 2009; Kin & Błażejowski 2013; Błażejowski *et al.* 2016; Trenchard *et al.* 2017). E, queuing behaviour observed in modern spiny lobsters (Herrnkind 1969). F, Fossil record of *Trimerocephalus chopini* queue (Błażejowski *et al.* 2016). Scale bar in F represents 10 mm.

FIG. 2. Three-dimensional modelling of the trilobite *Trimerocephalus chopini*. A, dorsal view. B, oblique anterior view. Scale bar represents 1 cm.

FIG. 3. Three-dimensional digital models of the trilobite *Trimerocephalus chopini*. A, dorsal view of one individual. B, oblique lateral view of one individual. C, oblique lateral view of four individuals in a queue. All scale bars represent 1 cm.

FIG. 4. Computational domain used in CFD simulations.

FIG. 5. Body of influence within the computational domain.

FIG. 6. Mesh used in CFD simulations, A, mesh in the computational domain. B, detail of the mesh within the body of influence. C, detail of the mesh near the head of one of the trilobite models. Scale bars represent: 5 cm (A); 3 cm (B); 0.3 cm (C).

FIG. 7. A, drag forces of trilobites in different positions in the queue of four individuals. B, percentage drag reduction of trilobites in the following positions (triangles show average drag reduction for all three followers).

FIG. 8. Drag coefficients of trilobites in different positions in the queue of four individuals. A, projected frontal area used as the characteristic area. B, total surface area used as the characteristic area.

FIG. 9. A, two-dimensional plot (vertical cross-section) of flow velocity magnitude for the queue of four individuals (inlet velocity of 2 cm s^{-1}). B, two-dimensional plot (vertical cross-section) of pressure for the queue of four individuals (inlet velocity of 2 cm s^{-1}). Direction of ambient flow from right to left. All scale bars represent 3 cm.

FIG. 10. A, percentage drag reduction of the first following trilobite at different distances from the leader and the excess drag reduction caused by the deceleration of the bottom boundary layer in the spacing between the follower and the leader in the queue of four individuals. B, excess drag reduction values interpolated over following distances of 0–48 cm at intervals of 0.1 cm. C, percentage drag reduction after subtracting the excess drag reduction. D, percentage drag reduction after subtracting

the excess drag reduction and the systematic error.

FIG. 11. A, drag forces of trilobites in different following positions in the queue of 20 individuals. B, drag coefficients of trilobites in different following positions in the queue of 20 individuals (projected frontal area used as the characteristic area). C, drag coefficients of trilobites in different following positions in the queue of 20 individuals (total surface area used as the characteristic area).

TABLE 1. Drag forces, drag coefficients and percentage drag reduction of trilobites in different positions in the queue of four individuals.

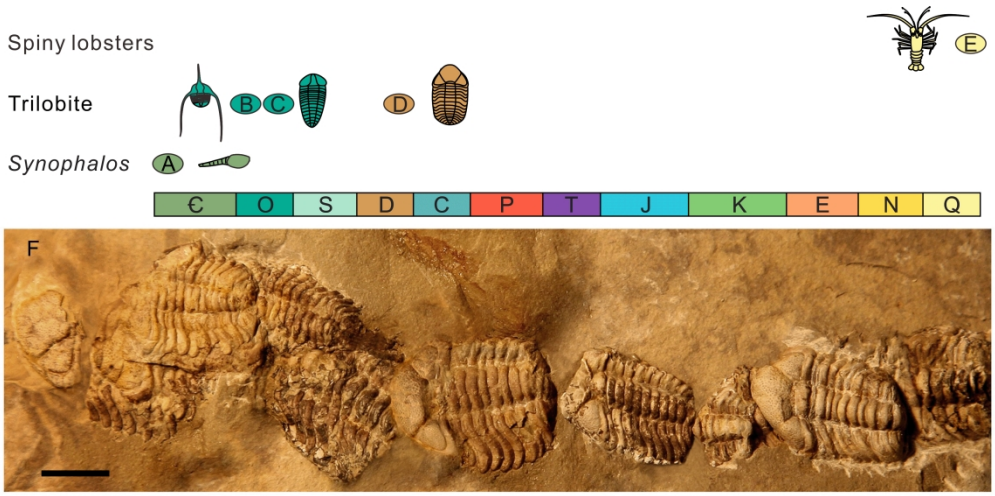

FIG. 1. Queuing behaviour in marine arthropods. A, chain-like associations of the putative crustacean *Synophalos xynos* from the Chengjiang Lagerstätte, China (Hou et al. 2009). B, queues of the trilobites *Agerina* and *Ampyx* from the Fezouata Shale, Morocco (Chatterton et al., 2008; Vannier et al., 2019). C, queues of the trilobites *Bathycheilus*, *Retamaspis* and/or *Salterocoryphe* from Portugal (Gutiérrez-Marco et al. 2009). D, queues of the trilobite *Trimerocephalus chopini* from Kowala Quarry, Poland (Radwański et al. 2009; Kin & Błażejowski 2013; Błażejowski et al. 2016; Trenchard et al. 2017). E, queuing behaviour observed in modern spiny lobsters (Herrnkind 1969). F, Fossil record of *Trimerocephalus chopini* queue (Błażejowski et al. 2016, pp. 3). Scale bar in F represents 10 mm.

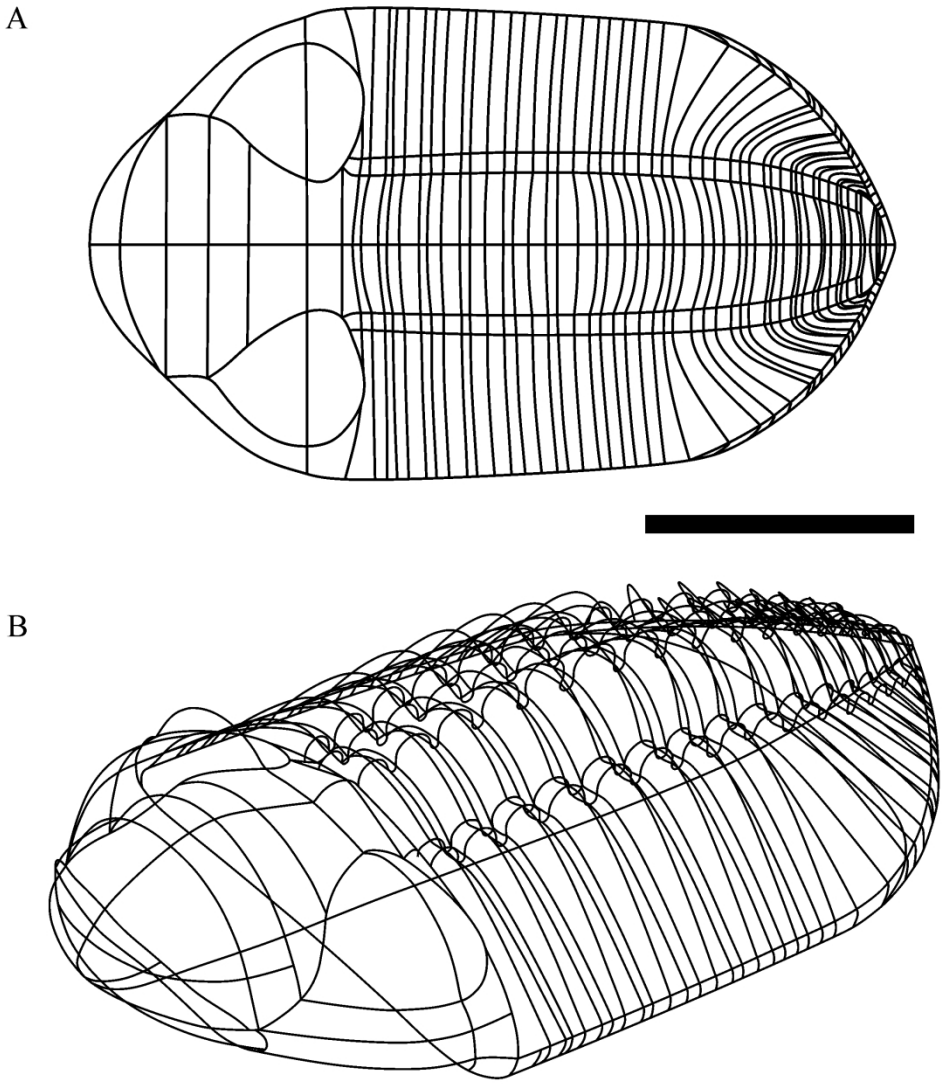

FIG. 2. Three-dimensional modelling of the trilobite *Trimerocephalus chopini*. A, dorsal view. B, oblique anterior view. Scale bar represents 1 cm.

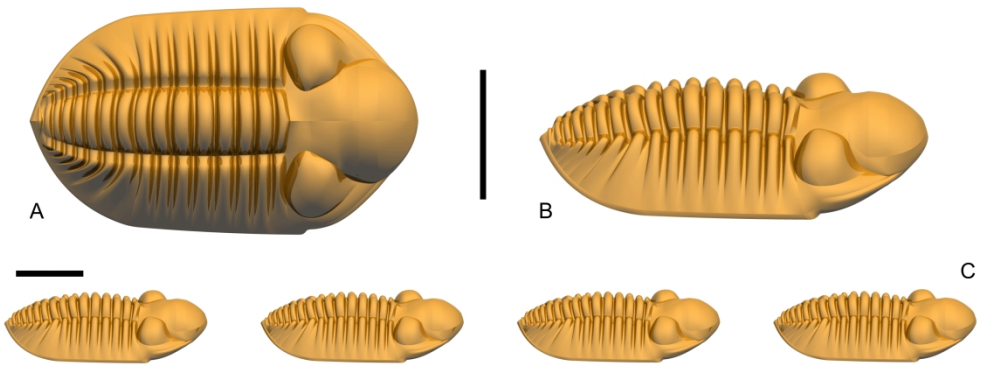

FIG. 3. Three-dimensional digital models of the trilobite *Trimerocephalus chopini*. A, dorsal view of one individual. B, oblique lateral view of one individual. C, oblique lateral view of four individuals in a queue. All scale bars represent 1 cm.

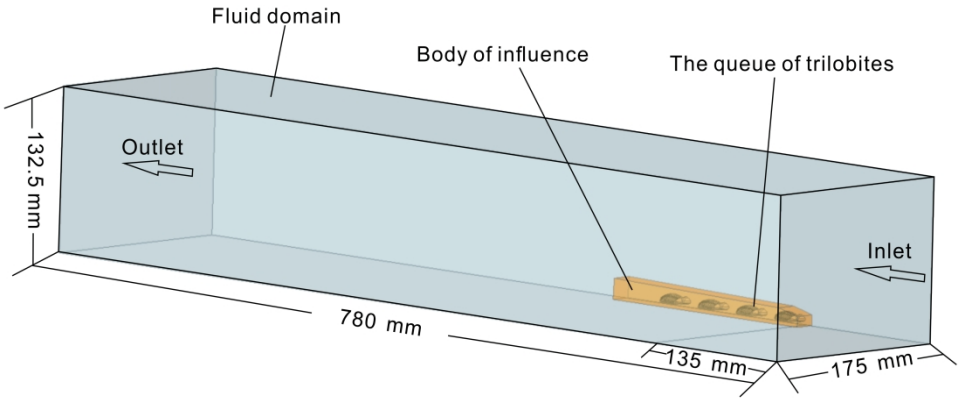

FIG. 4. Computational domain used in CFD simulations.

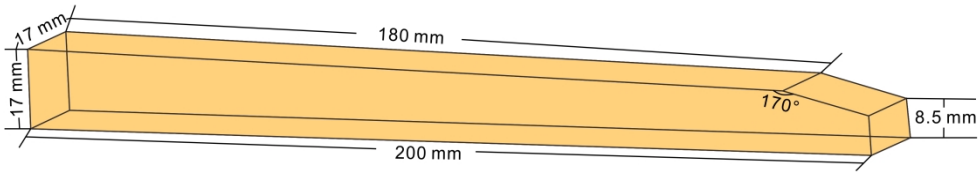

FIG. 5. Body of influence within the computational domain.

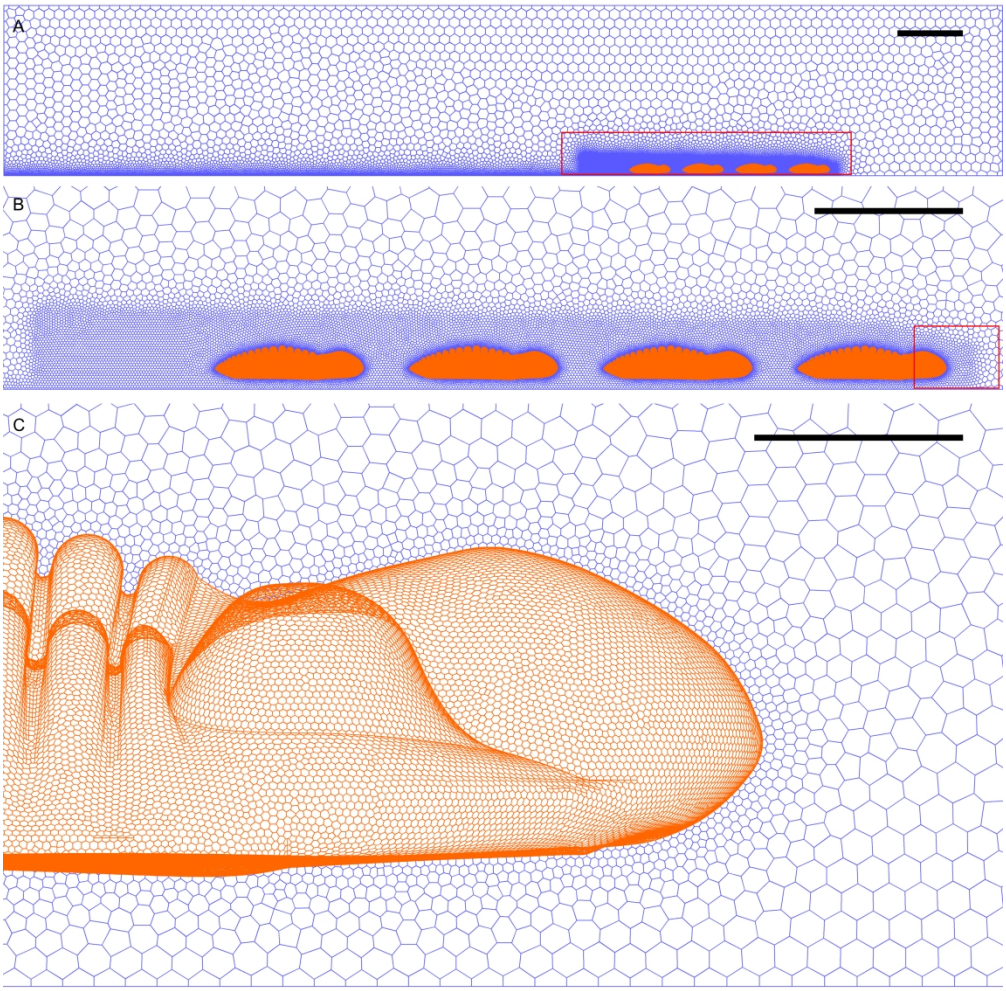

FIG. 6. Mesh used in CFD simulations, A, mesh in the computational domain. B, detail of the mesh within the body of influence. C, detail of the mesh near the head of one of the trilobite models. Scale bars represent: 5 cm (A); 3 cm (B); 0.3 cm (C).

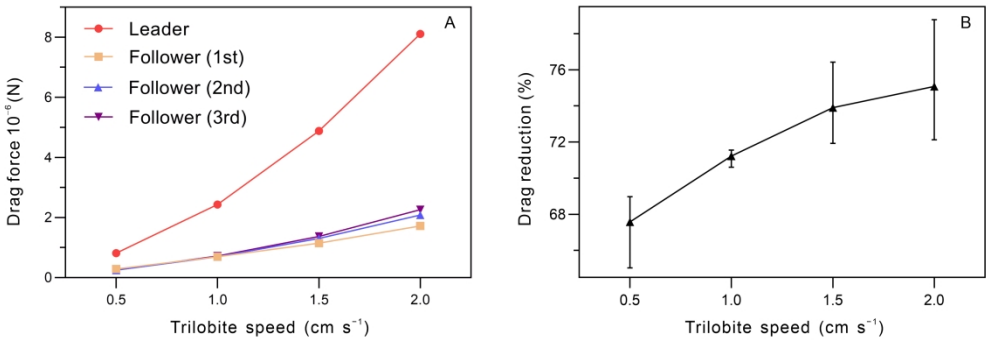

FIG. 7. A, drag forces of trilobites in different positions in the queue of four individuals. B, percentage drag reduction of trilobites in the following positions (triangles show average drag reduction for all three followers).

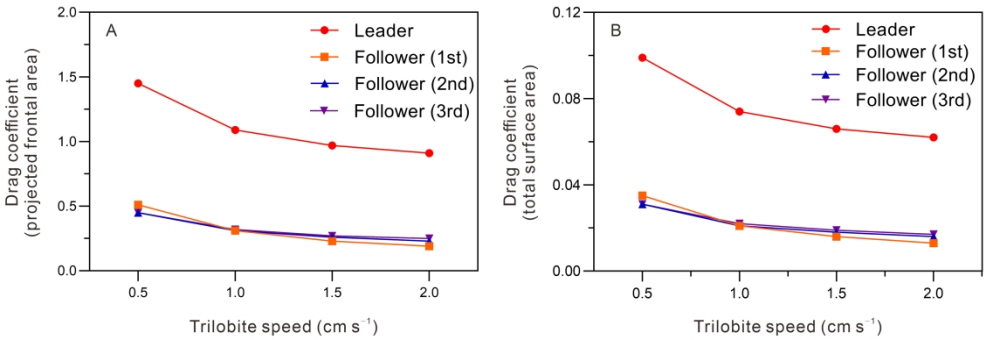

FIG. 8. Drag coefficients of trilobites in different positions in the queue of four individuals. A, projected frontal area used as the characteristic area. B, total surface area used as the characteristic area.

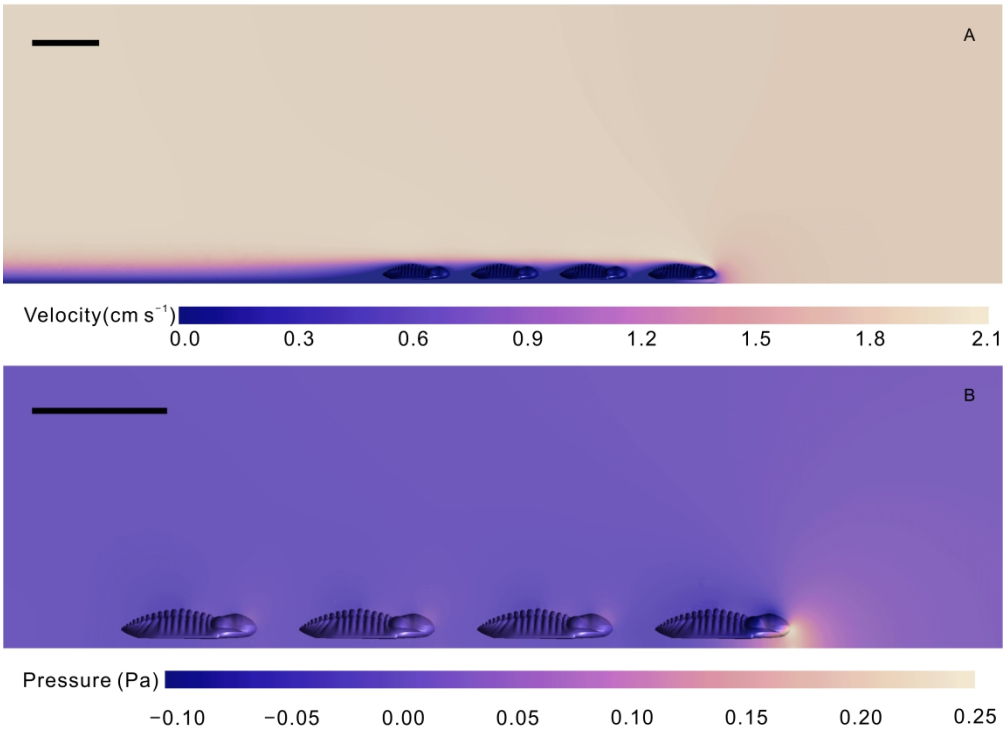

FIG. 9. A, two-dimensional plot (vertical cross-section) of flow velocity magnitude for the queue of four individuals (inlet velocity of 2 cm s^{-1}). B, two-dimensional plot (vertical cross-section) of pressure for the queue of four individuals (inlet velocity of 2 cm s^{-1}). Direction of ambient flow from right to left. All scale bars represent 3 cm.

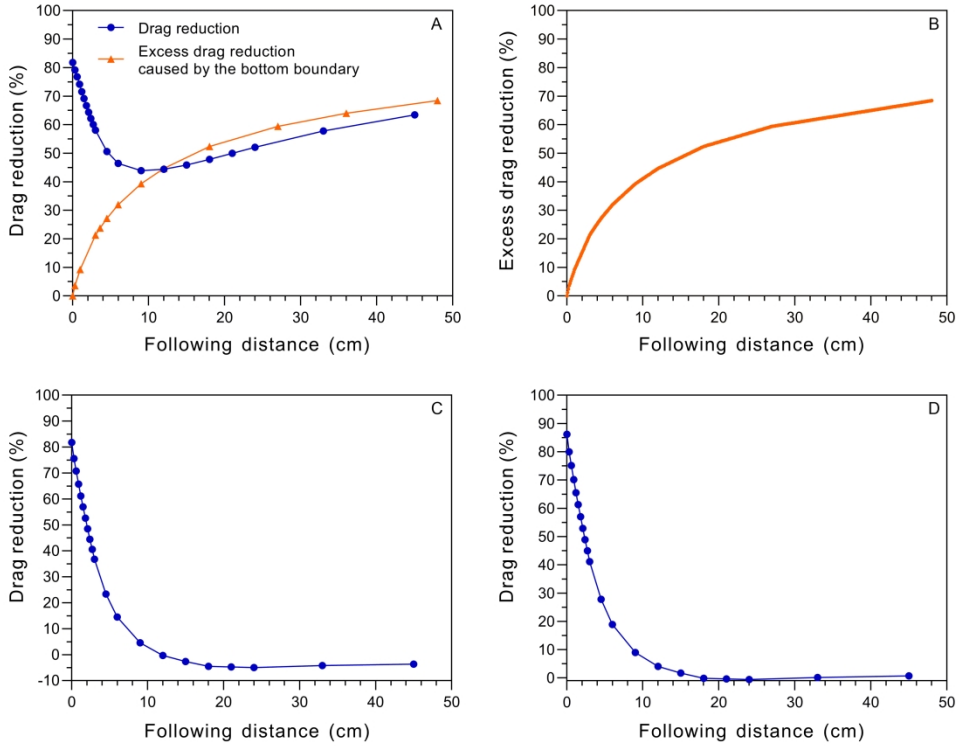

FIG. 10. A, percentage drag reduction of the first following trilobite at different distances from the leader and the excess drag reduction caused by the deceleration of the bottom boundary layer in the spacing between the follower and the leader in the queue of four individuals. B, excess drag reduction values interpolated over following distances of 0–48 cm at intervals of 0.1 cm. C, percentage drag reduction after subtracting the excess drag reduction. D, percentage drag reduction after subtracting the excess drag reduction and the systematic error.

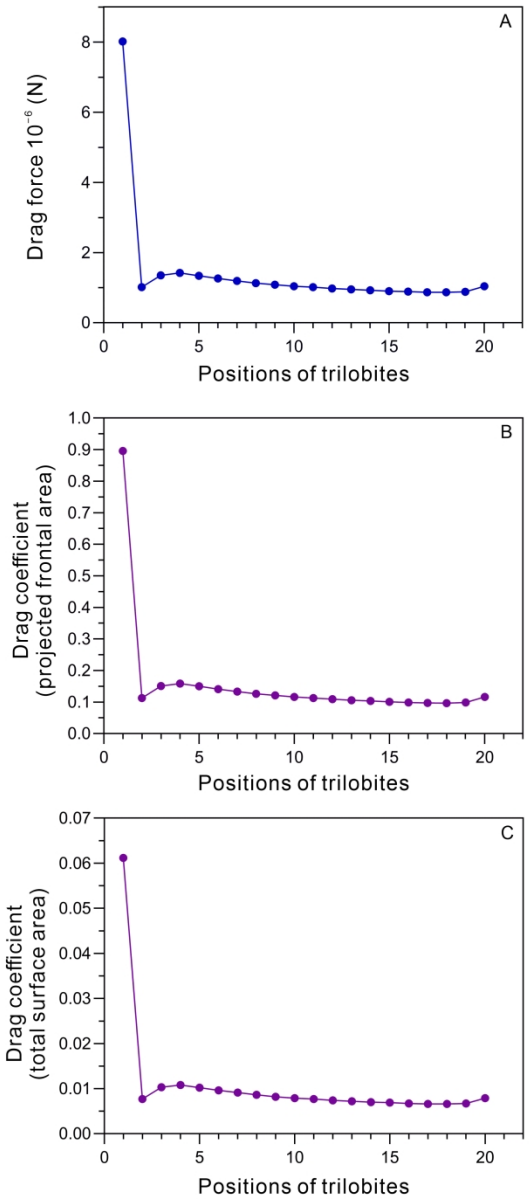

FIG. 11. A, drag forces of trilobites in different following positions in the queue of 20 individuals. B, drag coefficients of trilobites in different following positions in the queue of 20 individuals (projected frontal area used as the characteristic area). C, drag coefficients of trilobites in different following positions in the queue of 20 individuals (total surface area used as the characteristic area).

TABLE 1. Drag forces, drag coefficients and percentage drag reduction of trilobites in different positions in the queue.

Velocity (cm s^{-1})	Reynolds number	Position of the trilobite	Drag forces $\times 10^{-6}$ (N)	Drag coefficients (projected frontal area)	Drag coefficients (surface area)	Percentage drag reduction (%)	Error of percentage drag reduction (%) +	-
0.5	149	Leader	0.81	1.45	0.099	67.57	1.40	2.55
		Follower(1st)	0.28	0.51	0.035			
		Follower(2nd)	0.25	0.45	0.031			
		Follower(3rd)	0.25	0.45	0.031			
1.0	316	Leader	2.43	1.09	0.074	71.23	0.33	0.62
		Follower(1st)	0.69	0.31	0.021			
		Follower(2nd)	0.69	0.31	0.021			
		Follower(3rd)	0.71	0.32	0.022			
1.5	475	Leader	4.88	0.97	0.066	73.91	2.53	1.98
		Follower(1st)	1.15	0.23	0.016			
		Follower(2nd)	1.30	0.26	0.018			
		Follower(3rd)	1.37	0.27	0.019			
2.0	633	Leader	8.11	0.91	0.062	75.09	3.70	2.96
		Follower(1st)	1.72	0.19	0.013			
		Follower(2nd)	2.08	0.23	0.016			
		Follower(3rd)	2.26	0.25	0.017			